

Chilling a Feverish Planet using REHOS Technology

Unleashing High-Density Renewable Energy from Large Water Bodies like the Sea with Heat Recovery utilizing a REHOS Cycle

by

Johan Enslin

REHOS Product Designs

Abstract:

The successful development of a simplified AHT for use as chiller plant in an AWG application was recently patented by the AWG company. This led to the construction of a commercial prototype early 2021 and paved the way for full REHOS cycle deployment, making real contributions to mitigation of global warming.

The full REHOS cycle, where the developed AHT is regeneratively coupled to an ORC is modeled in this paper. Using this model of the binary ($NH_3 - H_2O$) cycle, process parameters were trended, highlighting the best practical range of operation where the thermodynamic cycle demonstrates the highest efficiency performance, summarized as: Input thermal energy ($5^\circ C < \text{Waste Heat Input } Q < 80^\circ C$) is converted in the REHOS cycle to delivering **15% of Q as power**, 10% of Q as hot water and 100% of Q as chilled water. The hot and chilled water may be mixed together, then **delivering 90% of Q as chilled output** with the power.

Seven divergent, extremely commercially lucrative example applications spell out the large commercial value of this REHOS technology with the serious potential of really chilling the globe in addition to drastically reducing CO_2 released into the atmosphere.

Index

- 1. Introduction**
- 2. Renewable Energy**
- 3. Recovery of Renewable Environmental Energy**
- 4. Absorption Heat Transformers (AHT)**
- 5. Centrifugal Reactor AHT Prototype Model**
- 6. AHT-ORC Coupling & the REHOS Cycle**
- 7. Example Applications:**
 1. The REHOS Chiller utilized for Electronics Cooling in a Data Centre
 2. REHOS Generator utilized for Utility P/S CW Heat Recovery
 3. A Mobile REHOS Charger for BEV's
 4. Large Mine Chillers using REHOS Technology
 5. A RAW-Pump utilized as Marine Propulsion Power Unit
 6. REHOS Generator extracting Energy from the Sea for H_2 Production
 7. A REHOS Chiller enhancing PV installations

1. Introduction

All energy on earth eventually contribute to heat the globe. Take the chemical energy in a liquid fossil fuel as an example. Solar radiation energy was used millions of years ago to capture carbon and build long carbon chains, trapping and preserving the solar energy deep underground. We now mine it, purify it and use the energy of combustion in an internal combustion (IC) engine. These engines are at best ~ 40% efficient, rejecting 60% of the chemical energy in the fuel as heat, back into the environment. The 40% energy available as shaft power, is used to propel a motor vehicle against friction in the bearings and air friction, converting all that engine power back to low grade heat of the environment....

Even the high-grade energy we know as electricity is generated in a fossil combustion (most likely coal fired) power plant with an efficiency ~ 35% and the balance of chemical energy in the coal is directly rejected into the environment. Transmission of the electricity convert a percentage (eg. 5 - 10%) to resistive heat in the power lines, and the electricity delivered to the actual user now only 25 - 30% of the original chemical energy in the coal, trapped inside a few million years ago. The user may use the electricity to power a number of electronic servers used for data computations in a Data Centre, where all the energy is gradually converted to heat in the electronic chips. This waste heat is removed by chilling plants, fans, coolers and air conditioning systems and rejected into the environment, heating the globe....

This is why man is striving to maximize conversion efficiency, so as to minimize the requirement to produce more energy, warming the planet. Using renewable energy however, break this cycle. Renewable energy is therefore that energy that would be absorbed on earth anyway (direct solar irradiation by the sun), or that have already been degraded to waste heat (giving rise to winds, waves and sensible heat in air and water). Using renewable energy therefore actually reduce the heating of the globe, effectively mitigating the global warming directly.

Nature is in balance, as CO_2 in the atmosphere is bound by photosynthesis to form part of green plants. Using active bio-material to produce fuels for combustion in various machines therefore does not upset the balance. Bio-material produced and stored deep underground as fossil fuels, however, upset this delicate balance and its combustion produce additional CO_2 , circulating the earth and shield radiant heat loss from the globe like a greenhouse, adding to heating the earth.

De-carbonization of all sectors of the industry have been happening way too slowly, and therefore earth is facing catastrophic warming, forcing us all to intensify efforts to accelerate de-carbonization of not only the power generation sector, but all sectors including mining, industry and the transport sector, namely land-, marine-, and air transport.

The UN drive for mitigation of global warming and de-carbonization to keep the planet temperature rise < 2°C (but preferably < 1.5°C) above pre-industrial levels is said not to be possible unless we do something drastically in the next 10 year window. All countries around the globe are called up to assist with policies and solutions to aggressively drive de-carbonization.

2. Renewable Energy

Total solar energy reaching earth as proportion of global human energy production was highlighted by Manowska & Nowrot in their 2019 publication [11]. They conclude that in the year 2000, man produced ~ 0.0414% of the total heating effect of solar irradiation reaching earth. This can also be written as the solar energy received on earth from our sun is 2415 times what the total global energy production by man was in the year 2000. The same figures for the year 2017 is 0.0577% or 1733 times human energy production. This not only show us how vast the renewable (solar) energy availability is, but also highlight the huge increase in man-made earth heating effect during the past 2 decades....

Using this solar irradiance for converting directly to electricity is one option, but not without challenges, though. Every conversion process we use for generating electricity needs a certain land area, and taking the total lifecycle energy production into consideration, it is also required to calculate land areas for producing the feedstock (mining for fossil combustion and fuel crops for biomass). These spatial footprints give us an idea of the power generation density applicable to generators we have become used to.

Spatial footprints of power output from various power generators as detailed by Cheng & Hammond [10] published in 2016 and some findings are listed below:

Coal combustion	3.63 - 4.00 km^2 / TWh	calculating to 262 $kWh / m^2 .annum$
LNG combustion	0.09 km^2 / TWh	calculating to 11100 $kWh / m^2 .annum$
Nuclear Power	0.3 - 0.5 km^2 / TWh	calculating to 2500 $kWh / m^2 .annum$
Wind Power	1.15 - 44.17 km^2 / TWh	calculating to 44 $kWh / m^2 .annum$
Solar PV	16.17 - 20.47 km^2 / TWh	calculating to 55 $kWh / m^2 .annum$
Biomass Power	470 km^2 / TWh	calculating to 2 $kWh / m^2 .annum$

Note that the area footprint for Solar PV and Wind generation is some 50 times the area requirement for Nuclear Power. Spatial footprint of coal fired power is also much larger than nuclear, as the coal mining operation area requirement also form part of the coal fired power generation spatial footprint. Biomass need the largest land area, as the cultivation of the feedstock use very large agricultural fields.

This low power density of solar PV and Wind power is the reason renewable energy is said to produce "dilute electricity", compared to Gas and Nuclear. On top of this, solar irradiation varies tremendously across the globe, noting that a one (1) kWp PV panel in the UK on average deliver ~ 750 kWh/a but ~ 1680 kWh/a in South Africa. South Africa is thus endowed with a very high solar irradiance, making the renewable solar power very cheap relative to Europe.

3. Recovery of Renewable Environmental Energy

Solar Cells convert the photon-energy in the sun's rays directly to electricity, and coupling a number of cells together in a solar (PV) panel has the advantage of not using any moving parts, however, the energy density is low as a result of the low solar irradiation falling on earth.

Solar energy may also be used indirectly, in conversion systems like Solar Thermal-, Wind-, and Wave Power, but all these conversions suffer from low energy density. Other indirect renewable energy concepts are also used, eg. Long Term Storage energy recovery like Tidal, Ocean Thermal (OTEC), Heat Pumps delivering hot water for domestic use as example. Although OTEC systems generate power from the thermal stored energy in the sea, the conversion efficiency is extremely low and the high capital investments required to increase the scale for greater economy make this type of renewable energy somewhat in-accessible.

Heat pumps may be used to extract sensible heat from the environment (cooling it down in the process) but it use expensive external energy (eg. electricity) to pump heat. The conventional vapor compression (VC) heatpumps generally use electricity to pump heat. Typical electricity usage of a VC heatpump for extracting thermal energy from ambient water and dissipating it into the air, chilling the water down to a temperature just above freezing, amount to ~ 8.2% (as a minimum) of the thermal heat load. This means that extracting 100 kW thermal energy from an ambient water source, would use 8.2 kWe to achieve that.

4. Absorption Heat Transformers (AHT)

Absorption heat transformers (AHT) use much less electricity, as the heat pumping action is actually powered by thermal energy. It uses electricity only for internal liquid pumping, being a few orders of magnitude smaller than the energy requirement of a vapor compressor as used in the VC heatpump. Much more details of the history and development of the simplified AHT was published by Enslin [2] in January 2019.

More recently, a simplified AHT pilot plant was constructed and tested in 2020 specifically for the purpose of ironing out all the teething challenges for the commercial use as VC replacement air chiller in an atmospheric water generator (AWG). For details, see the recent report on Pilot testing viability of Simplified

AHT for AWG use reported by Enslin & Murray [1], published February 2021. Typical performance as a function of the temperature lift or "upgrade" from the source (waste) heat input temperature for this application is presented in the graph of figure 1. In this graph the real thermodynamic efficiency calculated as:

$$COP_{AHT} = \frac{Heat_Pumped}{Energy_Used} = \frac{Q_{Lift}}{(Q_{Ambient} - Q_{Chilled})} \quad \{1\}$$

Note the value decrease with increasing temperature lift, but has a value > 0.7 for temperature lift values less than 40°C. For cascaded stages of AHT where the upgraded heat from the first stage is used as input heat for the second stage, the overall COP values decrease, as the values are calculated as:

$$COP_{Cascade} = COP_{Stage_1} * COP_{Stage_2} \quad \{2\}$$

and for identical performance the cascade value is simply the square of the single stage performance.

Figure 1

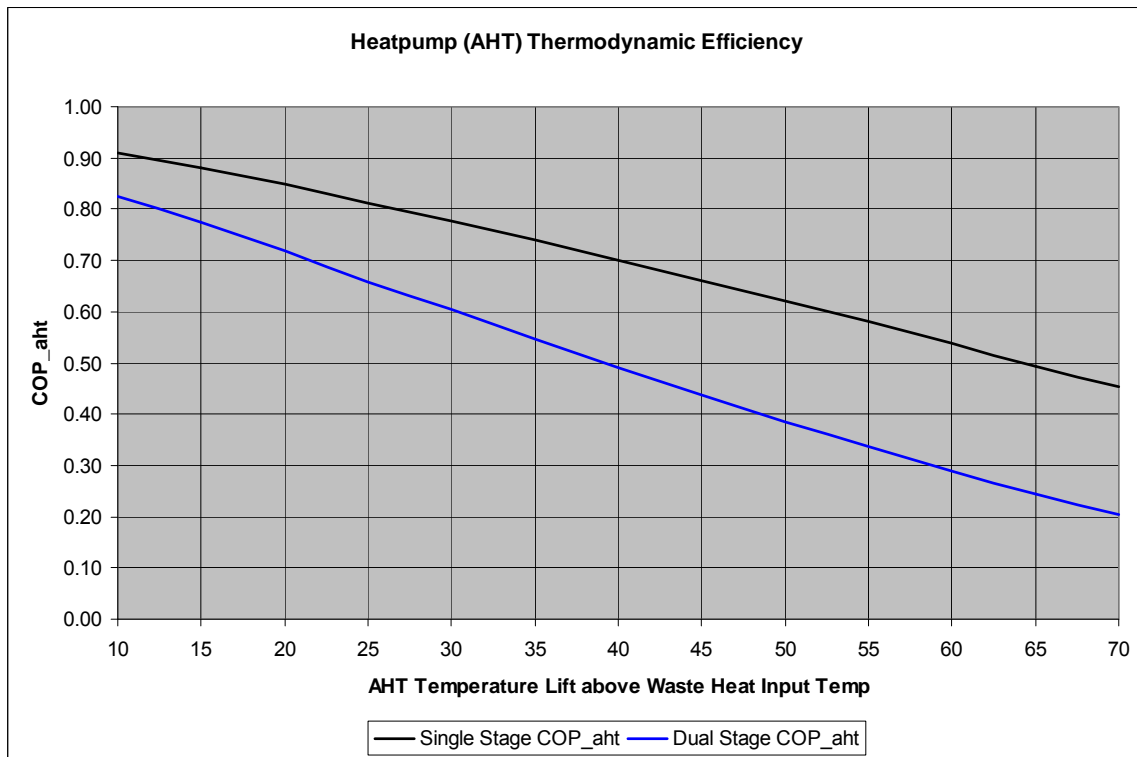


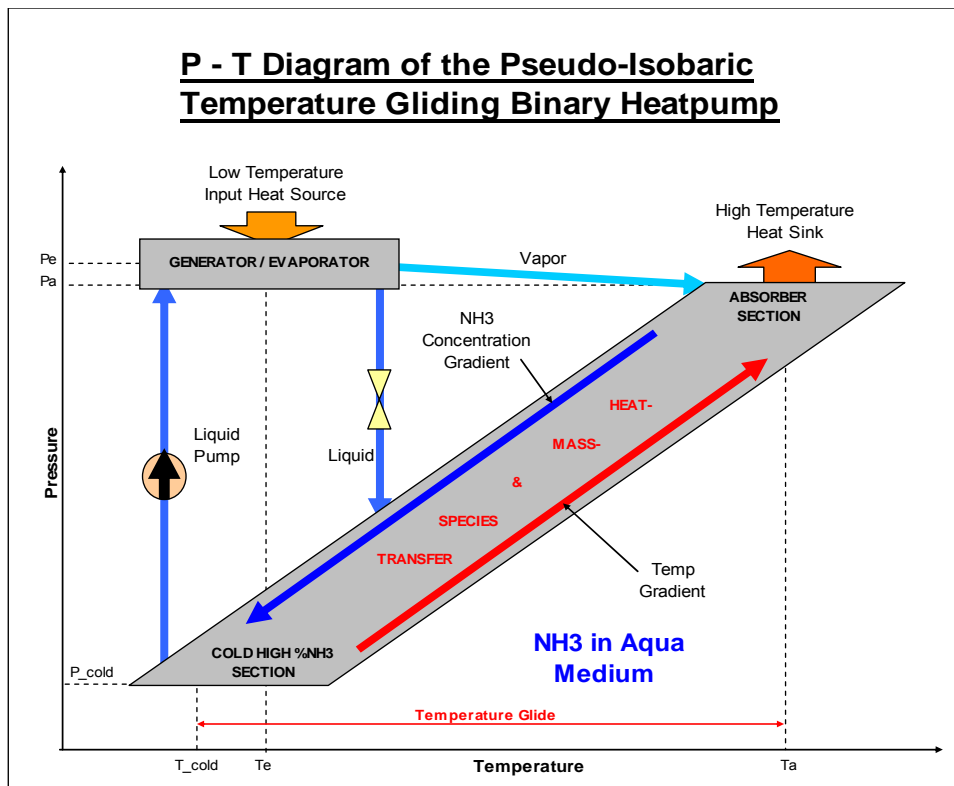
Figure 2 represent a pressure-temperature diagram of the simplified AHT.

The simplified AHT is sketched as a pseudo-isobaric temperature gliding bubble reactor fitted with an evaporator operated at a slightly higher pressure to facilitate spontaneous vapor flow from the evaporator to the absorber section of the

bubble reactor. Vapor generated in the evaporator is absorbed in the absorber section of the bubble reactor, generating heat that raises the temperature. Most of this heat is removed from the absorber in a H/E coil, (high temperature heat sink), while the remaining heat is used in the reactor to power the isobaric, temperature gliding distillation (NH₃ concentrating) endothermic process. The ammonia-rich liquid mixture at the cold end of the bubble reactor is pumped to the slightly higher evaporator pressure.

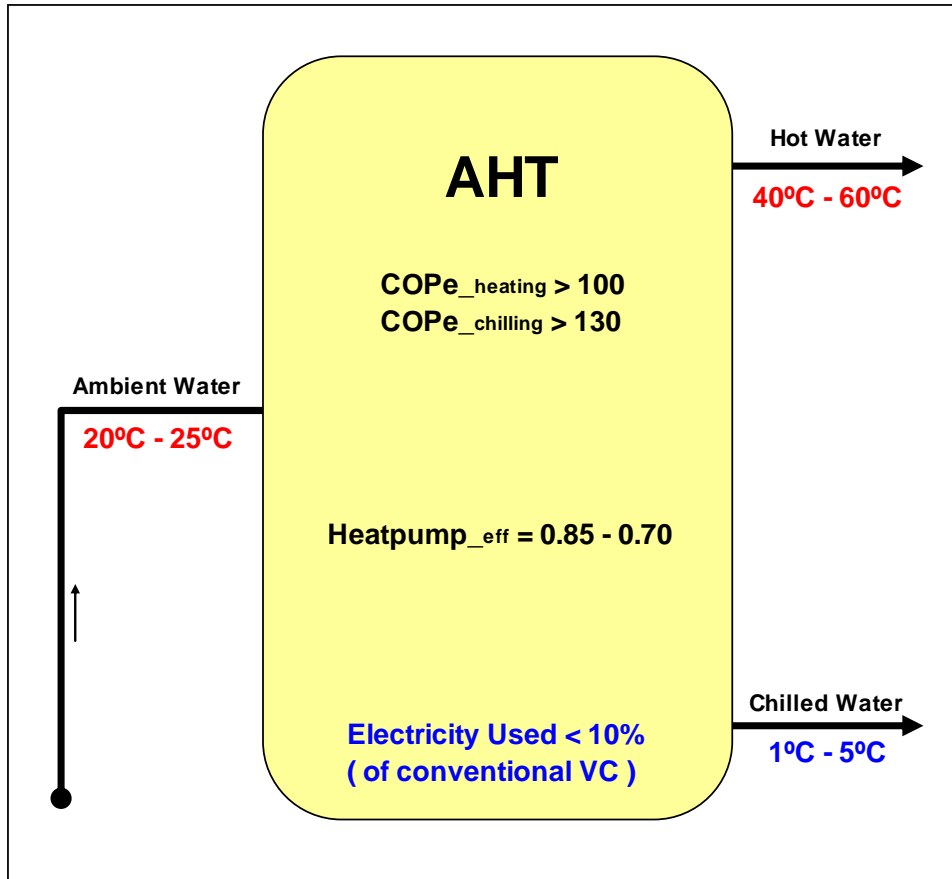
Although heat input into the evaporator is sketched in figure 2 as a single arrow into the evaporator, it is actually a flow process, where the waste heat source water (@ ambient temperature) flows into the evaporator, and as a result of heat being extracted from this liquid stream, the liquid exit stream is chilled to a much lower temperature. This is more visible in the simplified block diagram of the AHT as sketched in figure 3.

Figure 2



In figure 3, it is clear that in this simplified AHT, ambient temperature water is used as input (sensible) heat source, and due to heat extraction in the evaporator, this ambient water stream is chilled down to low temperature water output. Some of the extracted heat is used internally for the distillation process, and the balance is delivered as heated water output at the upgraded or "lifted" temperature. Because the internal distillation process utilize some of the extracted heat to power the process, the AHT efficiency or COP is always a value below 1, as we noticed also in the performance graph of figure 1.

Figure 3

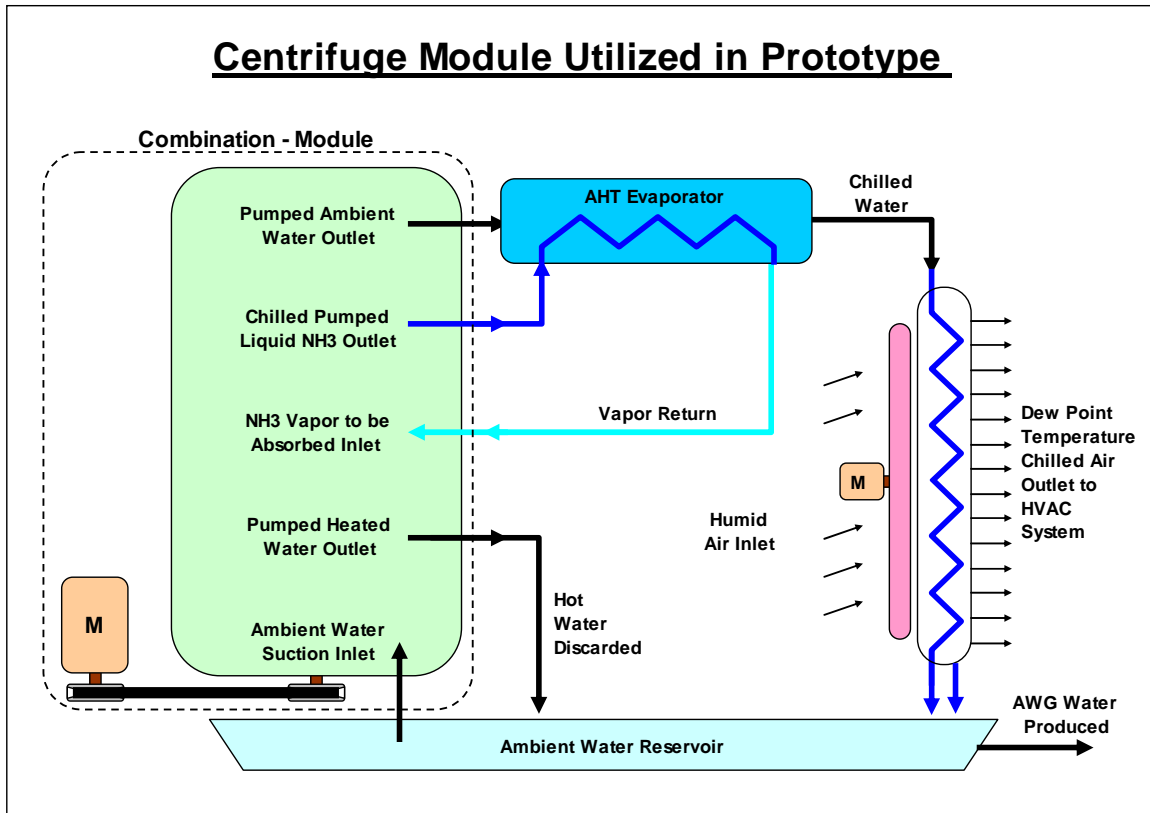


The most important aspect of the AHT is the very low electricity requirement. It actually use the thermal energy in the water to power the heat pumping process, and electricity is only used to power the liquid pumps, generally some two orders of magnitude smaller than a vapor compressor.

5. Centrifugal Reactor AHT Prototype Model

The pseudo-isobaric bubble reactor utilize the density difference in a zeotropic binary mixture of $\text{NH}_3 - \text{H}_2\text{O}$ between a hot, low NH_3 concentration liquid and a colder, higher NH_3 concentration liquid in a gravity field. Much higher rates of density separation is possible using a centrifugal force field instead of gravity, so the prototype commercial AWG unit we are constructing use a centrifugal reactor instead, as sketched in figure 4. This concept have several advantages over the standard vertical gravity-dependent pilot model we tested, as we were able to integrate various pumps including the water distribution pump with the rotating absorber and bubble reactor. This simplify the total AHT plant substantially, and is also physically smaller due to higher rates of H/E in the direct contact distillation column.

Figure 4



Note, however, that the hot water generated by the AHT is simply discarded and mixed with the chilled water after AWG use for complete energy balance purposes.

Before detailed design is possible, it is required to build a model in software (Microsoft Excel used here) to be able to calculate the energy flow and heat balances in the various components forming the complete process. This soft model also allow scenario testing and graph generation before the physical construction is started.

To model the process, it was required to generate two separate sets of lookup tables for the $NH_3 - H_2O$ binary mixtures used. A set of tables was generated for the mixture process parameters encountered at various different value constant pressure operations, as well as a separate set for various constant % NH_3 in the binary mixtures. These were made possible deriving it and correlating with the work of Ganesh & Srinivas [9] published in 2017.

The distillation column in the centrifugal field was modeled by dividing it into 10 annular liquid ring segments, spread radially outwards from the centre of rotation with stepwise (10 steps) increased diameters. The pressure in each segment was calculated as the previous (smaller diameter) segment pressure added to

the centrifugal pressure of the liquid column formed by the radial thickness of the segment. The saturation pressures so calculated therefore increased stepwise in 10 steps from the rotation centre to the outer periphery.

The NH₃ concentration was assumed to be increasing linearly from the hot absorber section at the outer periphery radially inwards to the colder section near the centre of rotation. With both the (saturation) pressure and the NH₃ concentration fixed, all the other parameters (including the temperature) could be obtained using the lookup tables for constant pressure. Vapor inflow from the outer periphery and liquid outflow in counter flow from the centre of rotation made the calculations dynamic and with mass-, as well as species- balance done in each segment sequentially, heat balance could be established in each segment by iteratively changing the mass of heated, lower %NH₃ counter flow liquid leaving each segment flowing radially outwards. The accumulated mass ratio of heated liquid radial outflow, to the condensing vapor radial inflow increase gradually with segment diameter, and reach a value of ~ 40:1 at the outer peripheral absorber section. Close to the absorber section where the heated liquid temperature is fairly high, a cooling water coil is inserted to remove the heat generated by the condensing vapor being absorbed into the liquid mixture. This 40:1 recirculation value in the distillation section, gave very stable and realistic performance values, also generating very realistic void fractions persistent in each segment.

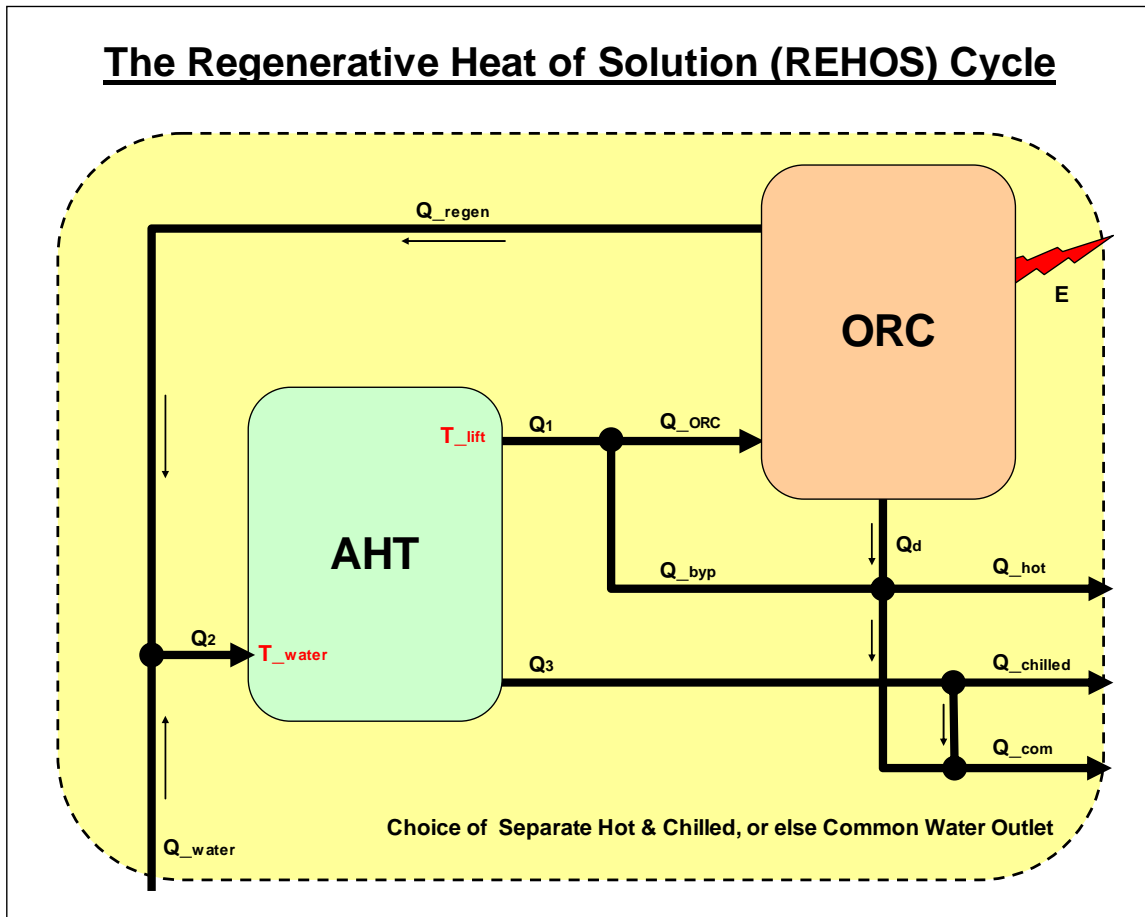
Using this balanced distillation column also facilitated very simple overall mass-, species-, and energy balance in all other components of the AHT and the add-on equipment. It also present the opportunity to make use of the heated CW outlet water for generating some power in an external ORC.

6. AHT-ORC Coupling & the REHOS Cycle

In this soft model the hot water is not simply discarded, but it is used to power an organic rankine cycle (ORC) for the generation of power. A portion of this hot water is used for powering the ORC, may also be bypassing the ORC completely to be able to calculate the pure AHT performance only. The percentage hot water used for ORC is designated as a parameter (Z) for calculations, to make it easy to evaluate performance using different values of Z without the need to change any formulas. The soft model can be graphically represented as process layout in figure 5 below. The different energy flows in the various flow stream lines were named by the letter Q with a specific name added as subscript. This make the labelled values in the formulas easily referenced on the process layout of figure 5.

Figure 5 actually forms a graphical representation of the novel, patented REHOS Cycle, which is an AHT coupled fully regeneratively to an ORC, for the generation of power. Heat rejection of the power generation unit as a whole is done via a chilled water outlet, and the REHOS cycle does not need any condenser.....

Figure 5



The symbols added to the sketch in figure 5 are used throughout this description for formulas and calculations. Energy input to the AHT is calculated as $(Q_2 - Q_3)$

$$COP_{AHT} = \frac{Q_1}{(Q_2 - Q_3)} = \frac{Q_1}{Q_{input}} \quad \{3\}$$

and the hot AHT output water carry energy Q_1 at the upgraded temperature T_{Lift} which is higher than the ambient temperature T_{Water} . By definition, the heat available to the ORC is:

$$Q_{ORC} = Z \cdot Q_1 \quad \{4\}$$

and

$$Q_{byp} = (1 - Z) \cdot Q_1 \quad \{5\}$$

Overall energy balance:

$$Q_{Water} = E - Q_{com} \quad \{6\}$$

Should you attempt to get the maximum power from a flowing stream of hot water using an ORC, a certain amount of heat is unavailable due to the H/E

pinch temperature you have to use. Using the zeotropic binary mixture as medium, however, allow some temperature gliding, absorbing more heat from the hot stream and lowering the unavailable heat from the hot source. This unavailable heat we designated as Q_d and may be calculated as the difference between the ideal carnot efficiency power and the real ORC power generated E.

$$Q_d = Z.Q_1.(1 - \frac{T_{Water}}{T_{Lift}}) - E \quad \{7\}$$

The ORC heat rejection is used as regenerative heat, added to the ambient input water heat Q_{Water} :

$$Q_{regen} = Z.Q_1 - E - Q_d \quad \{8\}$$

Heat balance around the liquid output node:

$$Q_{com} = Q_{byp} + Q_d + Q_3 \quad \{9\}$$

AHT input node heat balance:

$$Q_{Water} = Q_{input} - Q_{regen} \quad \{10\}$$

Incorporating formula {8} into equation {10}:

$$Q_{Water} = Q_{input} - Z.Q_1 + E + Q_d \quad \{11\}$$

Incorporating formula {3} and {6} into equation {11}:

$$Q_{Water} = \frac{Q_1}{COP_{AHT}} - Z.Q_1.(1 - \frac{T_{Water}}{T_{Lift}}) \quad \{12\}$$

ORC efficiency calculation:

$$\eta_{ORC} = \frac{E}{Z.Q_1} \quad \{13\}$$

and defining a fraction X which is a function of the specific media (refrigerant) used inside the ORC as well as the temperature range of operation. This factor normally range between 80% - 90%, and for the NH_3 mixture we use, we have assumed the value of X = 85%.

$$\eta_{ORC} = X.\eta_{CAN} \quad \{14\}$$

where the subscript "CAN" refer to the standard Curzon-Ahlborn-Novikov efficiency well known in the literature, representing the maximum ORC efficiency available, (using a single component refrigerant), working between the 2 mentioned temperatures:

$$\eta_{CAN} = (1 - \sqrt{\frac{T_{Water}}{T_{Lift}}}) \quad \{15\}$$

REHOS Cycle efficiency, defined as Power Output divided by the Heat Input:

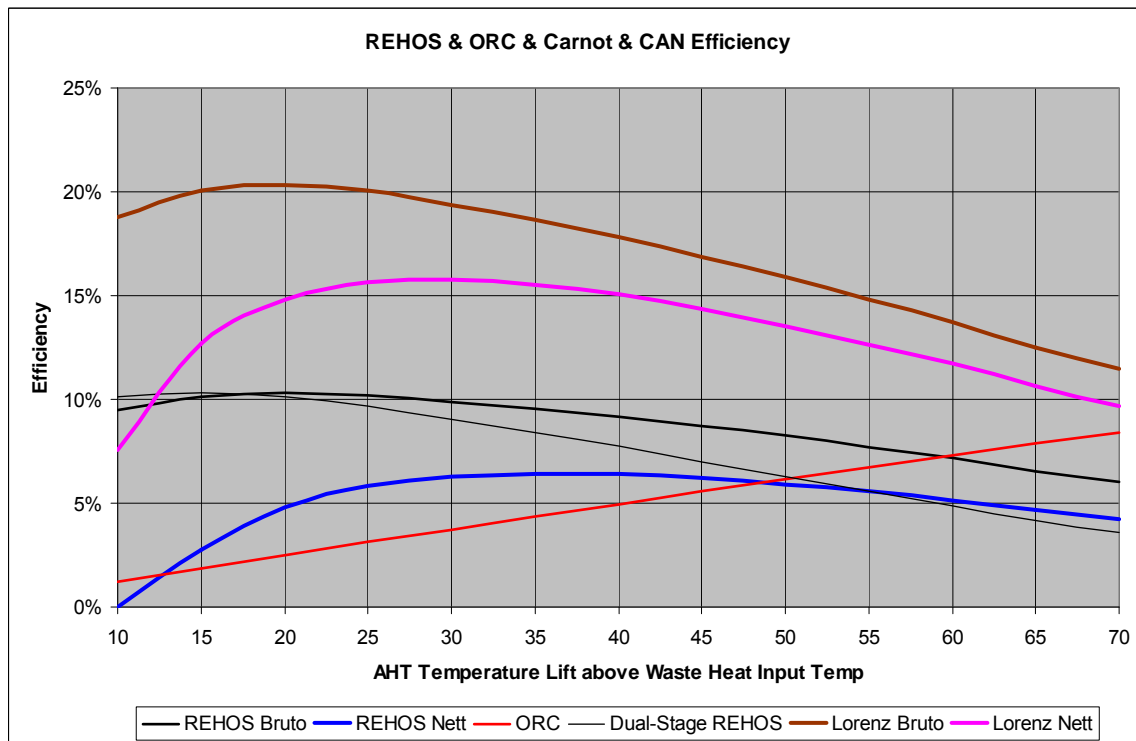
$$\eta_{REHOS} = \frac{E}{Q_{Water}} \quad \{16\}$$

Incorporating formula {13}, {14}, {15} and {12} into equation {16} :

$$\eta_{REHOS} = \frac{Z.X.(1 - \sqrt{\frac{T_{Water}}{T_{Lift}}})}{[\frac{1}{COP_{AHT}} - Z.(\frac{T_{Water}}{T_{Lift}})]} \quad \{17\}$$

The soft model was also used to trend some of the more interesting parameters in the REHOS Cycle as shown in figure 6. Note that for these trends of figure 6, parameter Z was set fixed at 100%, so maximum power is generated by the ORC and $Q_{byp} = 0$.

Figure 6



In this graph note the bruto REHOS cycle efficiency stay above 10% when the AHT temperature lift increase from 15°C to 30°C and drop to ~ 9.3% if the temp

lift increase further to 40°C. The REHOS netto power with all pumping, even CW circulation pumping subtracted, is very stable > 6% from a temp lift of 25°C to 50°C, and the maximum of ~ 6.4% @ a temperature lift of 35°C is very stable on a flat section of the curve. It is also much higher than the corresponding plain bruto ORC (the red curve) for the same temperature lift.

Note that the dual stage operation does not increase the power output efficiency, in fact it lowers the efficiency substantially with increasing temperature lift. This is due to the decreasing and much lower dual stage COP_{AHT} as we have already seen in the AHT performance curve of figure 1, also generated by the same soft model.

These curves was made with ambient input temperature of 20°C, making the average reactor pressure about 3 Bar Abs, but different values of ambient temperatures between 5°C - 55°C was also simulated and the results are nearly identical. With increasing inlet temperature the average saturation pressure just increase as @ 55°C the pressures run at 8 Bar Abs.....For REHOS cycles to be used at higher temperatures, it is recommended to use different zeotropic binary media eg. $LiBr - H_2O$ or other zeotropic refrigerant mixtures.

Using the model and formulas as listed, the various energy outputs may be written in terms of the Input energy (maintaining the temperature lift as 35°C) as follows using Z = 100% and X = 85%:

$$E = 6.4\% \cdot Q_{input} \quad \{18\}$$

$$Q_{hot} = 12.5\% \cdot Q_{input} \quad \{19\}$$

$$Q_{chilled} = 100\% \cdot Q_{input} \quad \{20\}$$

$$Q_{com} = 87.5\% \cdot Q_{input} \quad \{21\}$$

It is very useful to know that using a REHOS cycle (designed with separated media refrigerants for the AHT and the ORC) the power output as percentage of the thermal input energy is fairly constant at 6.4%, not dependent on the actual input energy temperature level.

Also, temperature levels of the outputs depend on the mass flow only, as the amount of thermal energy in the stream is fixed. As example let's assume the inlet temperature of a water stream is 20°C and the amount of thermal energy extracted from the stream (Q_{input}) is set at 100 kW. Should we need the chilled output water to be 5°C, we would throttle the chilled water outflow to 5.73 $m^3 / hour$, but if we are not really interested in so low chilling temperature, we could throttle the chilled water flow to 43.25 $m^3 / hour$ to deliver water at 18°C, only 2°C lower than the input water temperature. Similarly, as the hot water output is only 12.5% of the input energy, if we throttle the hot water line to 0.36

$m^3 / hour$, the hot stream temperature would be 50°C, but if we only need 30°C, we would throttle to 1.08 $m^3 / hour$ to achieve that.

All the above discussions, formulas and results assumed the ORC added to the AHT was added with isolated internal media, meaning that a different refrigerant may have been used in the ORC than the binary mixture used as media in the AHT. The heat transfer was done via H/E, isolating the media from each other. Should this not be the case, however, and the zeotropic binary media ($NH_3 - H_2O$) is used for both the AHT as well as the ORC, isobaric temperature gliding in the ORC evaporator as well as in the ORC condenser, convert the ORC into a Lorenz cycle. The effects have been very accurately documented in the thesis published by Jensen in 2015 [24] presented as part of his PhD degree. He has described that using the Lorenz effects within $NH_3 - H_2O$ binary mixtures the maximum power efficiency the ORC generate, is not limited to the Curzon-Ahlborn-Novikov efficiency as listed in formula {15}, but may in fact be some 110% - 130% of the ideal Carnot calculation!

Using a zeotropic binary mixture as media for the ORC, the isobaric temperature gliding of both the ORC evaporator and the ORC condenser (heat rejection), make the low temperature T_{water} not a single value, but rather the log mean of the two temperatures where condensing start and where it ends. Similarly, the high temperature T_{lift} is now calculated as the log mean of the temperatures where evaporation start and where it ends after gliding. The ORC efficiency first presented as formula {14} in our calculations should then rather be written as:

$$\eta_{ORC} = X \cdot \left(1 - \frac{T_{water}}{T_{lift}}\right) \quad \{22\}$$

using the log mean temperatures as mentioned and incorporating this into the REHOS efficiency calculation of formula {17} the REHOS-Lorenz efficiency may be calculated as:

$$\eta_{REHOS-Lorenz} = \frac{Z \cdot X \cdot \left(1 - \frac{T_{water}}{T_{lift}}\right)}{\left[\frac{1}{COP_{AHT}} - Z \cdot \left(\frac{T_{water}}{T_{lift}}\right)\right]} \quad \{23\}$$

With any specific NH_3 concentration in the ORC circuit, a specific saturation pressure used in the evaporator would allow the temperature gliding to produce an ORC efficiency equal to carnot efficiency using the original single values of temperatures T_{water} and T_{lift} . This make the calculation values using equation {23} correct in all cases. This brutto efficiency using equation {23} was also plotted on the graph of figure 6, as the brown "Lorenz Bruto" and with the internal

pumping, fan and water circulation pumping energy subtracted, the netto efficiency, plotted as the pink "Lorenz Nett" efficiency curve in figure 6. This drastically increase the REHOS power output values to > 15% in the range of AHT temperature lift between 20°C - 40°C. As more heat is used to generate this power, also the hot water outlet would be reduced by a few percent. The cycle output conditions as detailed in formula {18} - {21} may now be re-defined:

$$E = 15\% \cdot Q_{input} \quad \{24\}$$

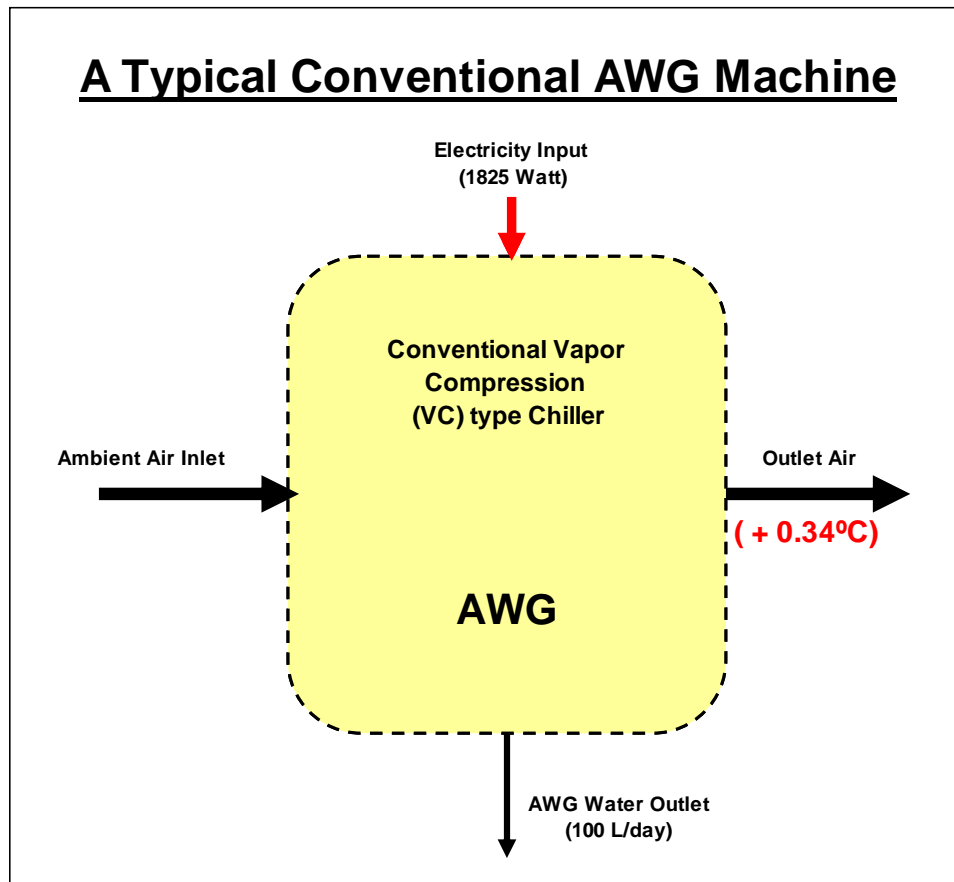
$$Q_{hot} \sim 10\% \cdot Q_{input} \quad \{25\}$$

$$Q_{chilled} = 100\% \cdot Q_{input} \quad \{26\}$$

$$Q_{com} \sim 90\% \cdot Q_{input} \quad \{27\}$$

These formulas {24} - {27}, were used exclusively for all subsequent illustrations and examples. It is just practical to use the higher power output available using the same zeotropic binary mixture for both the AHT and the ORC.

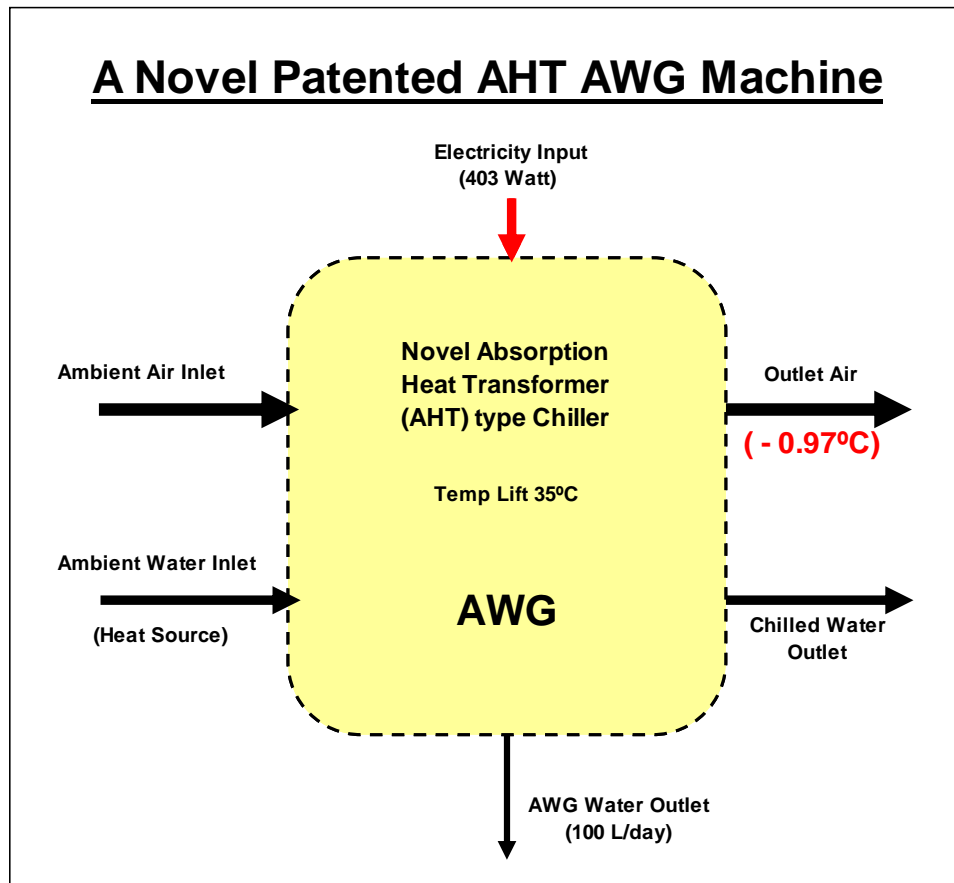
Figure 7



Should we compare the use of the REHOS cycle as chiller in an AWG water generator unit to the conventional VC chiller we note the overall energy balance:

With the conventional VC machine sketched in figure 7, the outlet air is slightly warmer than the inlet air (by $+0.34^{\circ}\text{C}$ in this example). Using the AHT as chiller, however, the scenario is slightly different. As you can see in figure 8, in addition to the air inlet and outlet, you also have ambient water inlet and chilled water outlet. The difference in temperature of the inlet and outlet water (energy levels) is used to power the chiller heat pump. The AWG unit use two H/E coils, however, one for cooling down the inlet ambient air so water can condense out, and another "hot" coil using any internal remaining energy to re-heat the air after the water have been removed. In figure 8, all remaining energy in the water streams are combined and used to re-heat the air. Even when all other temperatures are equal, energy balance with this AWG machine result in the outlet air at a slightly lower temperature (by -0.97°C in this example) than the input air.

Figure 8

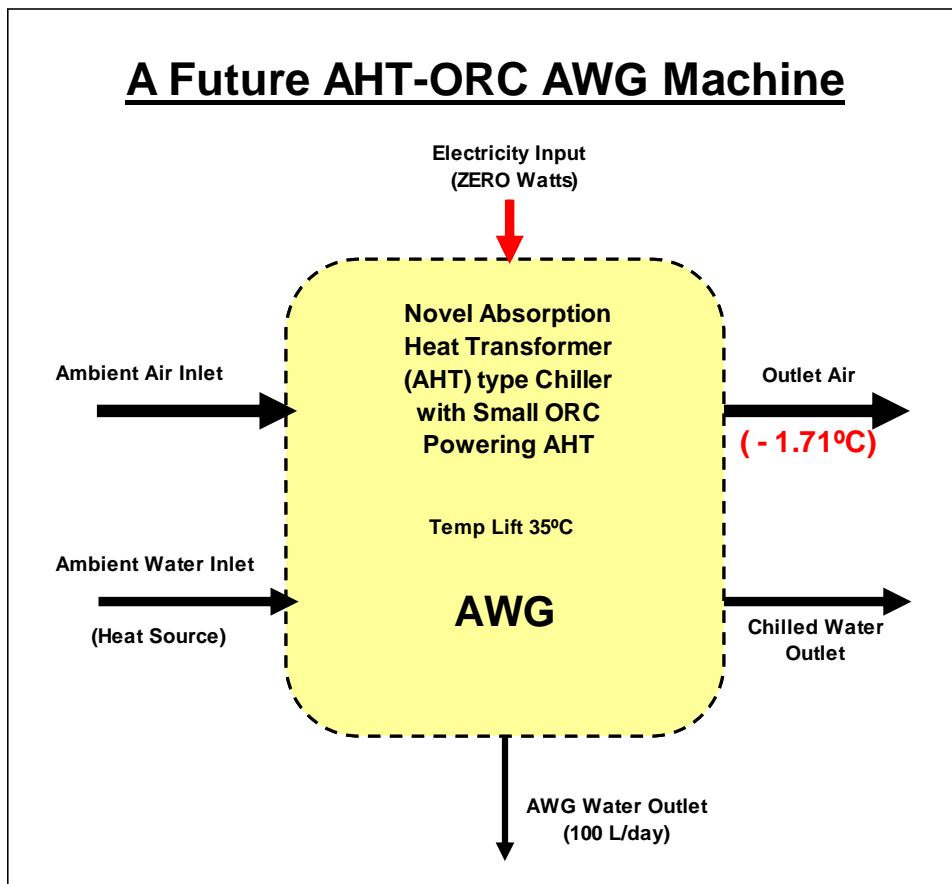


Should we add a small ORC (just large enough to provide pumping and fan energy to the AHT), making it totally external electricity-free, the outlet air chilling is even more pronounced. This is shown clearly in figure 9 with the outlet air chilled much more (to -1.71°C in this example). All other output stream energy is again equalized by adding the only temperature change from heat balance to the

outlet air temperature. Outlet hot as well as cold water streams are also recycled, combined to form the input water stream.

Power generated by the small ORC driven from the hot water stream is only large enough to provide the AHT with the required electricity to drive the liquid pumps and the air fan. In the formulas the value of parameter Z in this case had to be set to about 25%, bypassing some 75% of the hot water stream. This give a fully autonomous AWG operation, not requiring any external electricity, and would be very useful for providing water for human consumption as well as limited agriculture in extreme draught-stricken parts of the world. It is most definitely the future of AWG as it also bypass all the external electricity costs currently associated with the VC type chillers used in conventional AWG machines, dropping the cost of water production to be competitive with current municipal water supplies.....

Figure 9



Should we concentrate on maximizing the power output to produce an AWG machine, but also supply additional electricity that may be required eg. for water reticulation, pumping the water produced by the machine over long distances, we would set the parameter Z in our formulas to 100%. This allow the production of about 1 kW_e netto (conservatively for our example case) of electricity output for external use, with the 100 L/day AWG water produced.

Notice the large value of chilled air output (-3.71°C in this example machine), dropping below the ambient inlet air temperature as shown in figure 10. As the air flow through this AWG machines are quite high, the chilling effect of the output air is substantial, also helping to chill indoor air (part of air conditioning) in the warmer climate countries where this technology may be needed to provide potent water for human consumption due to draught and near-desert environmental conditions. A shopping centre utilizing this REHOS based AWG machine to provide potent water, may also provide chilled air for air conditioning (A/C) for the shopping centre, saving a tremendous amount of electricity use.....

The AWPG machine may very well become the future basis to draw power and water from the air for delivery to communities in remote area's far removed from the local electricity network grids, due to the modular, yet simple design easily mass-produced, chilling the globe wherever it is deployed. In the shopping centre example, this machine could deliver drinking water, A/C as well as some electricity to save more utility electricity bills!

Figure 10

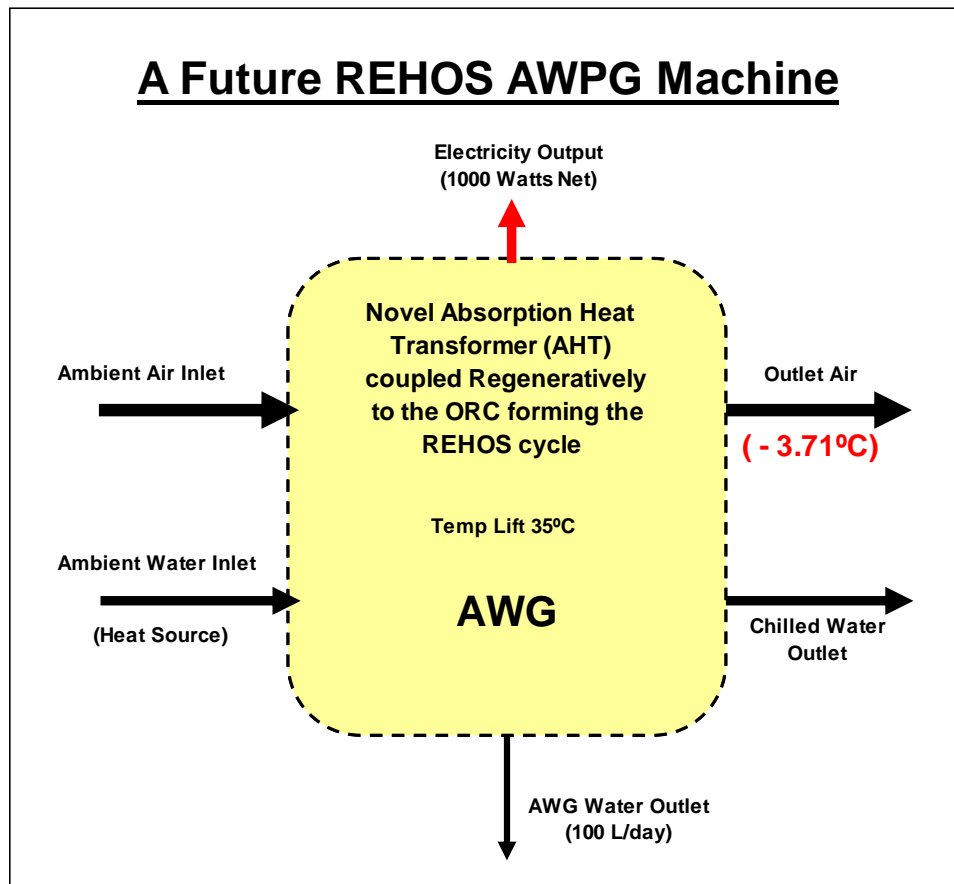


Figure 10 is an example of thermal energy extracted from the environment (the air) for use as power, cold as well as hot water. Thermal energy may of course

be extracted also from the environment as ambient water, using heat exchangers which are very much smaller (and cheaper) than H/E for heat removal from the air. A few example cases of practical uses are presented in section 7 to illustrate the versatility of the REHOS cycle, but the list is by no means exhaustive.

7. Example Applications:

7.1 REHOS Chiller utilized for Electronics Cooling in a Data Centre

This application focuses on the ability of the REHOS cycle to provide chilled water for cooling applications, replacing power-hungry A/C equipment to save money that would have been spent on electricity bills. Power is also recovered and added to the saving.

Some second generation ORC suppliers can now generate electricity economically from waste heat sources at a temperature as low as 80°C. Take Datacenter coolers as example. Datacenters are forced to use active coolers to dispose of all the heat generated by their servers and electronics packed into cubicles, as higher electronic computing speed and density heat up the chips and components to their maximum, currently limited to around 80°C. A typical Datacenter can pack servers and modules into a single cubicle with heat generating losses in excess of 16 kW, and if the Datacenter is very small, it may have 10 cubicles only, with the waste heat generated by these electronics already adding up to 160 kW of waste heat that need to be disposed. Using a conventional VC type chiller to do the cooling, would require ~ 8.2% of the heat to be removed, as electricity, and at a cost of R1-50/kWh, costs soar to R472-32 per 24 hour day, adding up to R172 397-00 pa. It therefore makes sense to look at alternative cooling strategies.

A certain cooling system supplier from Germany of second generation state-of-the-art ORC technology, can now convert this waste heat, at the ultra-low grade temperature below 80°C to electricity amounting to 8 kWe, to be credited on the Datacenter's electricity bill. With the high prevailing electricity price, the payback time for such an ORC system incorporated in the cooling strategy and financed from the savings, would be conservatively 5.5 years, even though the heat-to-power conversion efficiency is only 5%, as reported by Ebrahimi et al [1] in 2017.

The REHOS cycle we described, however, may supply chilled water as CW to the Datacenter, and as the water heats up in absorbing this 160 kW, recovering 15% (as per equation {24}) of this heat as power, therefore generating 24 kW of power to be additionally subtracted from the Datacenter supply power. The saving would therefore be the original cooling system electricity cost of R472-32 per day plus power sold as 576 kWh @ R1-50/kWh calculating to R864-00 per day. The total saving would therefore be R1 336-32 per day, adding up to R487 756-00 pa. or 23% of the actual electricity bill! This totally overshadows the already excellent German technology performance.

7.2 REHOS Generator utilized for Utility P/S CW Heat Recovery

In this application the REHOS cycle not only produce some 15% power (as per equation {24}) from the hot CW flow, but also create a chilled CW output to feed the condenser with near-ambient temperature to utilize all the REHOS cycle advantages to produce maximum power from the CW circuit of a conventional rankine cycle for profitable decarbonization of fossil combustion power generation.

Let's have a closer look at the CW circuit in a large utility scale dry-cooled power station (P/S) like Kendal of the electricity utility Eskom in South Africa. This pulverized coal fired P/S deliver 686 MW electrical power into the national grid at a thermodynamic efficiency of 42%. CW therefore remove 947 MW thermal energy from the condenser where the cold CW from the cooling tower enter the condenser at 34°C and leave at 48°C at MCR. The sheer volume of CW flow is staggering, and lend itself perfectly to modular, stepwise de-carbonization as follows:

Re-routing a pre-defined portion (66.7 MW) ultra-low quality waste heat at 48°C through a REHOS Generator would generate 10 MW electricity from it (15% as per equation {24}) and deliver CW chilled to below the required 34°C (closer to ambient temperature) to send back to the P/S condenser. The power generated represent a 1.46% saving on power needed to be generated by the station to produce 686 MW. Also, 1.46% fossil fuel combustion is avoided, obviously with the corresponding savings on the coal purchased, saving on ash removal and flue gas cleaning, as well as carbon credits resulting from the carbon footprint reduction. The cooling tower also need to dissipate 66.7 MW (7%) less heat into the environment. Kendal is dry cooled, but if it was a wet-cooled station, the water saving would also have been substantial. A wet-cooled coal-fired P/S of this size use $\sim 25\,000\ m^3 / day$ water, so the water saving would have been $\sim 7\%$ calculating to $1750\ m^3 / day$, regarded very highly in South Africa, as ours is a water-scarce country. As no fuel need to be purchased for the REHOS Generator, its operation is cheaper than the P/S rankine cycle, so adding this 10 MW heat recovery generator actually decrease the cost of generating power from this P/S. The implementation over time therefore become profitable as the working units pay for themselves in a very short time.

The chosen modular 10 MW REHOS Generator would be a small enough capital investment to be able to implement it from the annual maintenance budget, yet in only 7 steps already $> 10\%$ of the station power would be generated by recovered CW heat, requiring 10% less fossil fuel to be purchased. Installation is non-invasive to the rest of the P/S operation, and therefore does not require the station to be switched off, so the gradual, step-wise de-carbonization of the complete coal fired compliment of the utility power generation fleet will proceed

profitable, each unit providing additional monetary and environmental incentive to continue.....gradually over time reducing the carbon footprint of the P/S.

7.3 A Mobile REHOS Charger for BEV's

The REHOS cycle ability to extract thermal energy from the air via a chilled water coil and converting some of this energy into 15% power (as per equation {24}) is utilized in this application to generate mobile power for BEV charging, also while travelling to decrease battery requirements as well as electricity grid dependency for mobile BEV's in the transport sector.

A typical passenger motor vehicle shaped nicely aerodynamic, will have a drag coefficient of ~ 0.36 , and with a frontal area of $\sim 2.1 \text{ m}^2$ this vehicle would need:

@ 100 km/h => 10 kW power needed

@ 120 km/h => 17 kW power needed

@ 140 km/h => 27 kW power needed

The typical electric vehicle running off batteries (BEV) is therefore equipped with a 120 kWh battery to achieve a reasonable range of ~ 6 hours drive => 600 km.

Should we therefore develop a 15 kW REHOS mobile charger extracting thermal energy from the ambient air, at the delivery efficiency of 15% (as per equation {24}), the thermal energy required to be extracted would calculate to 100 kW. From our experience with AWG technology, the H/E required would have a air inlet area of only 0.91 m^2 , which can easily be accommodated on the vehicle roof. This H/E would be chilled with the produced chilled water at about 5°C to extract the heat from the air. Delivering 15 kW continuously, a battery is only required to provide the peak energy available for acceleration. The mentioned battery pack of 120 kWh may therefore be reduced to only 25%, or 30 kWh for the same driving achievement as the original BEV. This REHOS-Charged vehicle just need no external charging, and becomes totally self-sufficient, requiring no fuel and emit nothing into the environment!

A true revolution in mobility de-carbonization....

7.4 Large Mine Chillers using REHOS Technology

This application utilize the maximum chilling output, together with the maximum power generation (15% as per equation {24}) for chilled water reticulation in large electricity-free chillers to replace current power-hungry mine chillers and some of the water reticulation electricity requirements for the mining industry.

In the deep level mining industry chillers of sizes larger than 2 - 3 MW chilling capacity are common, and normally a number of chillers serve a single mine. Let's take the example of a deep level mine using 4 x 3 MW chillers on the surface at the mouth of the mine, pumping chilled water down into the mine and spending typically some 25% of the total mine operational costs on electricity for

chilling with a very large percentage of electricity use of the mine for water reticulation and pumping.

Should we assume three out of the four chillers run continuously in this example mine, requiring (some 8.2%) of 9 MW = 738 kW of electrical power, and at least twice as much for water and chilled water pumping. At the electricity purchase rate of R1-50/kWh, the 53136 kWh daily accumulation add up very quickly to an operational running cost of R 79704 per day....

A REHOS Chiller set would deliver the 9 MW chiller energy (as per equation {26}) and as by-product, also some 15% (as per equation {24}) power calculating to 32400 kWh and displacing the actual use of municipal power, saving R 48600 per day on the electricity bill.

Added together, the saving resulting from not using electricity for chilling of 17712 kWh and the REHOS power of 32400 kWh produce a operational saving of 50112 kWh or R 75168 per day, or 94% of the original mine (without REHOS chillers), chilling cost! What mine would not jump at the idea of replacing conventional chillers with REHOS technology generating a saving of R 27 Million annually, even if a part of this would finance the REHOS installation.....

7.5 A RAW-Pump utilized as Marine Propulsion Power Unit

In this application thermal energy extracted from a large water body like the sea is used as power source for propulsion purposes, removing the requirement of marine vessels to use a fossil fuel like diesel or bunker oil for propulsion. The term RAW-Pump refer to a REHOS Autarkic Water pump, where the thermal energy in the water is extracted and used to power a generator, as well as the pump that deliver this water as hydraulic energy (used for propulsion jets in this case).

Looking at the sea-going freighter benchmark ship of 13000 ton we notice power is produced in a large main diesel engine rated at 4.17 MW. This is supplemented by three auxiliary engines of 750 kW each, adding up to 2.25 MW. This make the total available power to the ship propulsion 6.42 MW.

As the ship's design speed is 13.3 knots and the average fuel index for HFO combustion is 3.15 g / (ton - mile), the average energy (41.5 MJ / kg) flow during the voyage suggest 7.225 MW of chemical energy input to the diesels. As the very large diesels convert the fuel into mechanical power with a thermodynamic efficiency of ~ 50%, the actual average real propulsion power used to travel at 13.3 knots calculate to 3.613 MW continuously.

Utilizing a few REHOS Generators to provide this power at 15% efficiency, the thermal energy that need to be extracted from the sea-water at 20°C calculate to 24.09 MW thermal, and assuming the H/E used will drop the water temperature by 2°C only, calculate to a water mass of 2878 kg/s or 10381 $m^3 / hour$. With

front-facing pipes for sea-water inflow at a velocity of 4.105 m/s (60% of the ship forward velocity of 6.842 m/s) and assuming we use 10 inlet pipes, the inlet pipes would only be 300 mm diameter.....

10 REHOS Generators of 361 kW power output each would take the place of the fossil combustion power plant, assisting hugely not only with money saving, but complete marine propulsion de-carbonization and chilling the global seawater at a rate of 19.27 MW thermal reduction (90% of 24 MW as per equation {27}). Adding this solution to most marine freight-moving vessels would make a real contribution in chilling our planet, not to mention the large reduction in CO_2 achievable.....all this on the revolutionary cost of fuel saving!

7.6 REHOS Generator extracting Energy from the Sea for H₂ Production

This application demonstrate the practicality of using the vast ocean as sensible heat reservoir for extracting thermal energy to generate power (some 15% as per equation {24}) from, exporting as H_2 and hydrogen carrying chemicals like NH_3 for the rapidly exploding global energy market. This energy carrier is seen as the major contributor for mobility de-carbonization, especially aero-mobility.

Using electricity for powering electrolizers commercially, we know the process need 60 kWh / kg H_2 but the current electrolizers are only 70% efficient, therefore needing 85.7 kWh / kg H_2 produced. This need a lot of renewable energy to produce Green Hydrogen on a commercial scale.

According to Dr Tobias Bishoff-Niemz (Enertrag South Africa CEO) in an article about the Hydrogen Economy called "Power-to-X" published in Engineering News of 26 Feb - 4 Mar, 2021, the global demand for green hydrogen would soar to 600 million tons/annum by 2050. South Africa is ideally endowed with renewable resources to capture some 5% to 10% of this market in H_2 exports, to earn some €50-billion in exports. As South Africa's GDP is only about €300-billion, this is a huge growth and is likely to create at least 500 000 jobs directly, not to mention the millions indirectly....

To capture 5% of this market, however, we need to produce 30-million tons of green hydrogen, requiring 2571-billion kWh / annum of renewable energy. Using solar PV and Wind require the spatial footprint land area of 55 and 44 $kWh / m^2 \cdot annum$ respectively, averaging 50 $kWh / m^2 \cdot annum$. This require a spatial footprint area of 51 429 km^2 , representing quite a large piece of land. Should we use REHOS Generator technology, however, the complete scenario change.

The REHOS generator may extract waste heat from the sea to produce power continuously (assume 7000 hours per annum). The size of machine required, would need to be 368 MW electrical, and at 15% conversion rate (equation {24}) the thermal energy it needs to extract from the sea would calculate to 2453 MW.

Considering the Koeberg nuclear power station in the Western Cape at full power discharge about $80 \text{ m}^3 / \text{s}$ of cooling water into the ocean at $\sim 10^\circ\text{C}$ higher than ambient. This represent a heat load dumped into the sea of 3341 MW. With this perspective, the REHOS plant suggested would use about 73% of the discarded heat of Koeberg to generate 368 MW electricity continuously for export in the form of H_2 . With no fuel needed, this installation would very soon pay for itself. This is a no-brainer that need to be pursued urgently....and we do not need to stop at 5% of this very lucrative green H_2 exploding international market. Modular, systematic smaller installations everywhere across South Africa next to large water bodies would certainly help to chill our feverish planet?

7.7 A REHOS Chiller enhancing PV installations

The REHOS cycle ability to extract thermal energy from the environment via a chilled water coil and converting some of this energy into 15% power (as per equation {24}) is utilized in this application to generate power, but at the same time, provide chilled cooling water for cooling down PV panels for efficiency increase, panel washing to remove dust as well as extracting atmospheric water from the air (AWG) to supplement the washing water volume in arid countries.

We know that PV panels are heat-sensitive, and should the panel temperature rise above 25°C , power output is degraded at the rate of its temperature coefficient, which in general for mono-crystalline silicon cells would typically be $0.5\%/^\circ\text{C}$. This result in a degrading in a hot desert-like environment at 45°C ambient of more than 10%. High solar irradiation areas normally also have a dust problem, so panel cleaning becomes critical to maintain the power output, but high irradiation areas very often also have a water shortage, making panel cleaning very difficult and expensive.

The conversion efficiency of large mass-produced PV panels are rarely $> 15\%$, although technologies progressively develop higher efficiency panels. Large utility-scale PV plants, however, make use of the older generation panels, as they require a lower capital outlay. Lets assume we have a 50 MWp PV installation made up from 200 000 PV panels of 250 Wp each (with conversion efficiency $\eta = 12.9\%$) in a fairly dry land area. Due to the low conversion efficiency, the major portion of the solar incidence is directly contributing to heating the panels, so waste heat is abundant in excess of 388 MW. The panels are therefore mounted off the ground to allow cooling natural airflow, and are mounted skew with some 20° with the horizontal, so dust will drop off and not accumulate on the panel. This plant perform mediocre, only for the 6 hours direct sunshine daily, but power drop off by as much as 2.5 MW during the hottest period in the day, due to ambient temperatures soaring.

To this plant, we add a number of REHOS Chillers, operated from a reservoir of ambient water to deliver 50 MW additional non-intermittent electrical power to the station. The thermal energy used, need to be extracted from the ambient water,

to the value of 333 MW (15% efficiency as per equation {24}), and chilled water at 5°C is also produced (equation {27}) to the value of 300 MW. This 5°C chilled water is pumped to the upper edge of the PV panel rows, and slots in the polyurethane piping allow chilled water to run over the face of the panels, not only cleaning it in the process, but also cooling it to average ~ 15°C. The water is then collected at the lower edge of the panel in a hollow plastic pipe collector (polyurethane pipe split open), from where it is accumulated and pumped back to the reservoir via a filter to remove the dust. The chilled water at 5°C (very often below dew point) washing over the accumulated large area of PV panels, also chill the air in immediate contact and condense some water from it into the chilled liquid film, accumulating with the washing water and supplement the water volume in the main reservoir.

With this addition, not only are dust removal challenges overcome, it also accumulate and supplement its own water from the atmosphere (AWG) and in addition generate an additional 50 MW of non-intermittent REHOS power (some of this obviously used for cooling water reticulation). Cooling of the PV panels increase the photovoltaic power generated by close to 5%, boosting photovoltaic power from the panels to 52.5 MW. The station output therefore ramp up from 50 MW during the non-sunshine hours, to 102.5 MWp during the 6 sunshine hours, but only 50% intermittent!

Again, a no brainer.....

Real commercially lucrative applications of REHOS technology are only limited by our own small imagination....and the more widespread this technology is deployment, the faster we can chill our planet.....

Selected Previous Publications:

1. The Wally-AHT Pilot AWG Development Project Joint Report, by Johan Enslin, Mike Murray and others was published in February 2021 on my website [http://www.heatrecovery.co.za/.cm4all/iproc.php/Wally-AHT Pilot AWG Development Project Joint Report.pdf](http://www.heatrecovery.co.za/.cm4all/iproc.php/Wally-AHT_Pilot_AWG_Development_Project_Joint_Report.pdf)
2. The document "Key Principles of the REHOS Cycle" was written by Johan Enslin in November 2018 and published in the Open Access Bioenergetics Journal at <https://www.omicsonline.org/open-access/key-principles-of-the-rehos-cycle-2167-7662-19-154.pdf> in January 2019, as well as on my own website [http://www.heatrecovery.co.za/.cm4all/iproc.php/Key Principles of the REHOS Cycle.pdf](http://www.heatrecovery.co.za/.cm4all/iproc.php/Key_Principles_of_the_REHOS_Cycle.pdf)
3. The document titled "Rankine Cycle efficiency increase by the Regenerative Recovery of Historically Rejected Heat" was written by Johan Enslin in October 2018 and published in the Open Access Bioenergetics Journal at <https://www.omicsonline.org/open-access/rankine-cycle-efficiency-increase-by-the-regenerative-recovery-ofhistorically-rejected-heatrev2-2167-7662-1000155.pdf> in January 2019 as well as on my own website [http://www.heatrecovery.co.za/.cm4all/iproc.php/Rankine Cycle efficiency increase by the Regenerative Recovery of Historically Rejected Heat_rev1.pdf](http://www.heatrecovery.co.za/.cm4all/iproc.php/Rankine_Cycle_efficiency_increase_by_the_Regenerative_Recovery_of_Historically_Rejected_Heat_rev1.pdf)
4. The document titled "Economic Aspects of Utilizing Heat Transformer Technology.pdf" was written by Johan Enslin in February 2019 and published on my website [http://www.heatrecovery.co.za/.cm4all/iproc.php/Economic Aspects of Utilizing Heat Transformer Technology.pdf](http://www.heatrecovery.co.za/.cm4all/iproc.php/Economic_Aspects_of_Utilizing_Heat_Transformer_Technology.pdf)
5. The follow-up document "Clarification of COP calculations for Absorption Heat Transformer (AHT) Type Heat Pumps.pdf" was written by Johan Enslin (to enhance the Executive Overview paper) in March 2018 and published on my website [http://www.heatrecovery.co.za/.cm4all/iproc.php/Clarification of COP calculations for Absorption Heat Transformer \(AHT\) Type Heat Pumps.pdf](http://www.heatrecovery.co.za/.cm4all/iproc.php/Clarification_of_COP_calculations_for_Absorption_Heat_Transformer_(AHT)_Type_Heat_Pumps.pdf)
6. The document titled "Comparison of various Modern Heatpump Technologies for unlocking Commercial Value from Ambient Heat_rev4.pdf" was written by Johan Enslin in April 2018 and published on my website [http://www.heatrecovery.co.za/.cm4all/iproc.php/Comparison of various Modern Heatpump Technologies for unlocking Commercial Value from Ambient Heat_rev4.pdf](http://www.heatrecovery.co.za/.cm4all/iproc.php/Comparison_of_various_Modern_Heatpump_Technologies_for_unlocking_Commercial_Value_from_Ambient_Heat_rev4.pdf)

7. These listed documents and many more published by the same author are also available for download from my website: [REHOS Product Designs](#)

References:

8. The Viability of Ultra Low Temperature Waste Heat Recovery using Organic Rankine Cycle in Dual Loop Data Centre Applications, by Khosrow Ebrahimi, Gerard F. Jones and Amy S. Fleischer and published in Applied Thermal Engineering 126 (2017) 393 - 406, made available by Elsevier.
9. Development of Thermo-physical Properties of Aqua-Ammonia for Kalina Cycle systems, by N. Shankar Ganesh and T. Srinivas published in the Int Journal Material and Product Technology Vol 55, Nos. 1/2/3, 2017.
10. Life-cycle energy densities and land-take requirements of various power generators: A UK perspective, by Vincent K. M. Cheng and Geoffrey P. Hammond, published by Elsevier in the Journal of the Energy Institute 90 (2017) 201-213 available from ScienceDirect and published online 18 February 2016.
11. The Importance of Heat Emission Caused by Global Energy Production in Terms of Climate Impact, by Anna Manowska and Andrzej Nowrot of the Silesian University of Technology in Poland, published 9 August 2019 in Energies 2019, 12, 3069; doi:10.3390/en12163069.
12. Void fraction, bubble size and interfacial area measurements in co-current downflow bubble column reactor with micro bubble dispersion, by Freddy Hernandez-Alvaro, Dinesh V. Kalaga, Damon Turney, Sanjoy Banerjee, Jyeshtharaj B. Joshi, Masahiro Kawaji published in Chemical Engineering Science 168, (2017) 403-413 made available by Elsevier.
13. Vortex Centrifugal Bubbling Reactor, by A.O. Kuzmin, M.Kh. Pravdina, A.I. Yavorsky, N.I. Yavorsky, V.N. Parmon published in Chemical Engineering Journal, 107 (2005) 55-62 made available by Elsevier.
14. Analysis of Absorber Operations for the 5 kW Ammonia-Water Combined Cycle, by Serisha Devi Govindaraju as Master of Science Thesis at the University of Florida, 2005.
15. Performance of Different Experimental Absorber Designs in Absorption Heat Pump Cycle Technologies:- Review by Jonathan Ibarra-Bahena and Rosenberg J. Romero published in the Open Access Journal, Energies 2014, 7, 751-766 in February 2014.

16. Ammonia-Water desorption in flooded columns, by James Hollis Golden for his Master's Thesis at the Georgia Institute of Technology in August 2012.
17. Multiscale multiphase phenomena in bubble column reactors: A review by Shuli Shu, David Vidal, Francois Bertrand and Jamal Chaouki, published in the journal *Renewable Energy* of 5 April 2019.
18. Development of a Heat Transfer Coefficient Model via Experimental Validation, by Adel A. Al-Hemiri and Nada Sadoon Ahmedzeki in the journal *Chemical Product and Process Modeling*, article 35 in Volume 3, Issue 1, 2008.
19. Review: Bubble column reactors, by Nigar Kantarci, Fahir Borak and Kutlu O. Ulgen published in the journal *Process Biochemistry* 40 (2005) 2263-2283.
20. Prediction of the Heat Transfer Coefficient in a Bubble Column Using an Artificial Neural Network, by Adel A. Al-Hemiri and Nada S. Ahmedzeki published in the *International Journal of Chemical Reactor Engineering*, article A72, Volume 6, 2008.
21. Hybrid Heat Pump for Waste Heat Recovery in Norwegian Food Industry, Stein Rune Nordtvedt (2005), Institute for Energy Technology, Instituttveien 18, N-2027 Kjeller Bjarne R. Hornotvedt, Hybrid Energy AS, Ole Deviks vei 4, N-0666 Oslo, Jan Eikefjord, John Johansen, Nortura AS, Rudshøgda, Norway, Stein.Nordtvedt@ife.no. (*This paper was published in the proceedings of the 10th International Heat Pump Conference 2011.*). This paper is also published as part of the IEA Handbook [2], page 57 - 61.
22. Thermally driven heat pumps for heating and cooling, compiled and edited by Annette Kühn (Ed.) as the Universitätsverlag der TU Berlin 2013, as the IEA Handbook available as handbook ISBN (online) 978-3-7983-2596-8 at email publikationen@ub.tu-berlin.de
23. Experimental Evaluation of a single-stage Heat Transformer used to increase Solar Pond's Temperature, by W. Rivera of Centro de Investigación en Energía-UNAM, P.O. Box 34, 62580, Temixco, Mor. , Mexoco and published in *Solar Energy* Vol 69, No. 5, pp. 369 - 376, 2000.
24. Industrial Heat Pumps for High Temperature Process Applications (*A numerical study of the ammonia-water hybrid absorption-compression heat pump*) by Jonas Kjaer Jensen, Ph.D. Thesis, Kongens Lyngby December 2015, DTU Mechanical Engineering, Technical University of Denmark.

25. Development of the Hybrid Absorption Heat Pump Process at High Temperature Operation, by Anders Borgås, Masters Thesis June 2014, NTNU Department of Energy and Process Engineering, Norwegian University of Science and Technology.
26. An Introduction to the Kalina Cycle, reprinted by Henry A. Mlcak, PE , first published in PWR- Vol.30, Proceedings of the International Joint Power Generation Conference, with editors: L. Kielasa and G.E. Weed, Book No. H01077-1996.
27. Energy saving into an absorption heat transformer by using heat pipes between evaporator and condenser, by M.I. Heredia, J. Siqueiros, J.A. Hernández, D. Juárez-Romero, A. Huicochea, J.G. González-Rodríguez, 15 September 2017 and published in Applied Thermal Engineering 128, (June 2018), 737 - 746.
28. Upgrading of Solar Heat by an Absorption Heat Transformer assisting with a Vapor Compression Heat Pump, by Nattaporn Chaiyat and Tanongkiat Kiatsiriroat of Maejo University, Chiang Mai, Thailand, May 2014.
29. Absorption heat transformers - A comprehensive review, by Kiyan Parham, Mehrdad Khamooshi, Daniel Boris Kenfack Tematio, Mortaza Yari, Uğur Atikol, 31 March 2014, and published in Renewable and Sustainable Energy Reviews 34 (2014), 430 - 452.
30. The Viability of Ultra Low Temperature Waste Heat Recovery using Organic Rankine Cycle in Dual Loop Data Centre Applications, by Khosrow Ebrahimi, Gerard F. Jones and Amy S. Fleischer and published in Applied Thermal Engineering 126 (2017) 393 - 406, made available by Elsevier.